

22/75

Nature, Distribution & Origin of Clay Minerals in Grain Size Fractions of Sediments from Manganese Nodule Field, Central Indian Ocean Basin

V PURNACHANDRA RAO & B NAGENDER NATH

National Institute of Oceanography, Dona Paula, Goa 403 004, India

Received 3 June 1987; revised received 26 February 1988

DT, IR and X-ray diffraction analyses have been carried out on 3 grain size fractions (< 1 , 1-2 and 2-4 μm) of sediments from the Central Indian Ocean Basin. Results indicate that there are 2 smectite minerals (montmorillonite and Fe-rich montmorillonite). Montmorillonite is present in all size fractions of sediments, whereas Fe-rich montmorillonite is present only in < 1 and 1-2 μm fractions of siliceous and $< 1 \mu\text{m}$ fractions of pelagic clays. Distribution of clay minerals suggests that illite, chlorite and kaolinite are the detrital products from Ganges and Brahmaputra and montmorillonite is derived from the weathering of the ridge rocks. Fe-rich montmorillonite in siliceous and pelagic clays is a result of early diagenetic processes. Size fraction studies suggest that montmorillonite tends to crystallise in $< 2 \mu\text{m}$ size range.

Clay mineral distribution in the surficial sediments of the Indian Ocean¹⁻⁵ indicates that the sediments are largely detrital in origin. The nature and abundance of smectite is important among clay minerals because, apart from the detrital smectites, authigenic smectites are also reported in the deep sea environment⁶⁻⁸ and the smectite being smallest in size⁹, its distribution tends to change with size of the sediment. Nature and origin of clay minerals as a function of grain size from different depositional environments has not been studied in the Indian Ocean. This paper presents the nature, distribution and origin of clay minerals in grain size fractions from the surficial sediments of the Central Indian Ocean Basin (CIOB).

CIOB ($5.7 \times 10^6 \text{ km}^2$) is in the Indian Ocean bordered by the ridge systems with 90°E Ridge on the east, Mid-Indian Ridge on the west and SE Indian Ridge on the south. Its northern portion is open towards Indian peninsula and its northwest extension is bordered by Chagos-Laccadive Ridge. Terrigenous, siliceous and pelagic clay sediments are dominant in the basin, whereas calcareous sediments are present adjacent to the ridge system.

Materials and Methods

Thirty two sediment samples (Fig. 1), collected in the CIOB by the Peterson grab, during 1983-85 from different cruises of *M V Skandi Surveyor* and *M V Farnella* were studied. Polymetallic nodules were associated with these sediments.

X-ray diffraction studies—Sediment samples were oven dried at 60°C, made free of salts and dispersed in ammonia solution. Later these samples were ana-

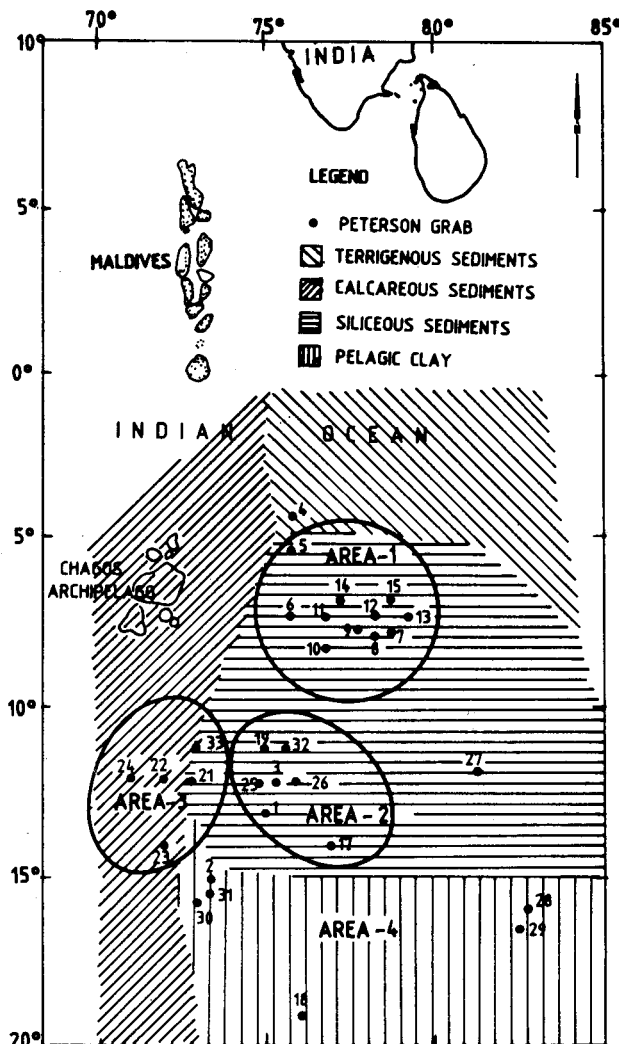


Fig. 1—Sample location map

lysed for texture¹⁰. Clay ($< 2 \mu\text{m}$) was separated from all the samples and made free of CaCO_3 and organic matter by treating with acetic acid and H_2O_2 respectively. Two oriented slides for each sample were prepared by pipetting the clay solution on glass slide and air dried. These samples were analysed on a Philips X-ray diffractometer using Ni-filtered Cu K_α radiation operated at 20 mA and 40 kV from 3° to $30^\circ 2\theta$ at $2^\circ 2\theta.\text{min}^{-1}$. The same sample was treated with ethylene glycol at 100°C for 1 h and X-rayed using the same instrumental settings. The clay minerals were then identified¹¹ and the areas of their first order reflections were measured above the baseline from the glycolated X-ray diffractograms. Percentage of clay minerals was calculated and crystallinity of montmorillonite was measured based on the ratio of the height of the peak above the background (P) and the depth of the valley (V) on the low angle side of the peak¹².

Two representative samples from each of the environments (Fig. 1) 11 and 13 from siliceous, 29 and 31 from pelagic and 21 and 22 from calcareous were studied for the mineralogy of the size fractions. These sediments were dispersed in ammonia solution as described above and the fractions < 1 , 1-2 and 2-4 μm were separated using Stoke's settling velocity principle and used in analyses.

Clay fractions were X-rayed and the percentage of clay minerals and the crystallinity of montmorillonite were calculated¹². Duplicate analyses show that the results are accurate within 10% for montmorillonite and within 5% for illite and kaolinite plus chlorite. The lesser accuracy for montmorillonite results from the problem of drawing base line. Crystallinity of illite¹³ is calculated measuring the width ($\Delta 2\theta$) at half peak height of the (001) diffraction peak of illite and comparing it for all size fractions with respect to the sediment type.

Infrared and DTA studies—Sediment fractions (< 1 and 1-2 μm) were made free of carbonates by treating with acetic acid and washing with distilled water to remove the acid and dried. These powders were thoroughly mixed with spectrally pure K Br¹⁴, transferred to the steel die and pressed into a disc under vacuum at 15 tonnes pressure for 2 min. The discs were placed in Uni-Cam spectrophotometer and scanned from 400 to 4000 cm^{-1} . Several trials were made using different thickness of the discs, so that the best possible spectral bands were obtained.

DTA was carried out for $< 2 \mu\text{m}$ fraction of the sediments using DTA-O₂ Universal from 0° to 1000°C at $7.5^\circ\text{C}.\text{min}^{-1}$.

Results

Distribution of clay minerals in $< 2 \mu\text{m}$ fraction—Clay minerals such as montmorillonite, illite and

kaolinite + chlorite are present in order of abundance. The texture of sediments varies from silty clay to clayey silt in area 1 and is clayey silt in areas 2 to 4 (Fig. 1).

Percentage of montmorillonite varies from 18-22, 28-32, 25-28 and 33-38 in areas 1 to 4, respectively, while the percentage of illite ranges from 46-51, 35-40, 49-51 and 33-36 in these areas.

Kaolinite + chlorite percentages did not show any trend in different areas. The estimation of kaolinite + chlorite was difficult owing to the interference of (020) reflection of phillipsite and (050) reflection of clinoptilolite.

Nature and distribution of clay minerals in size

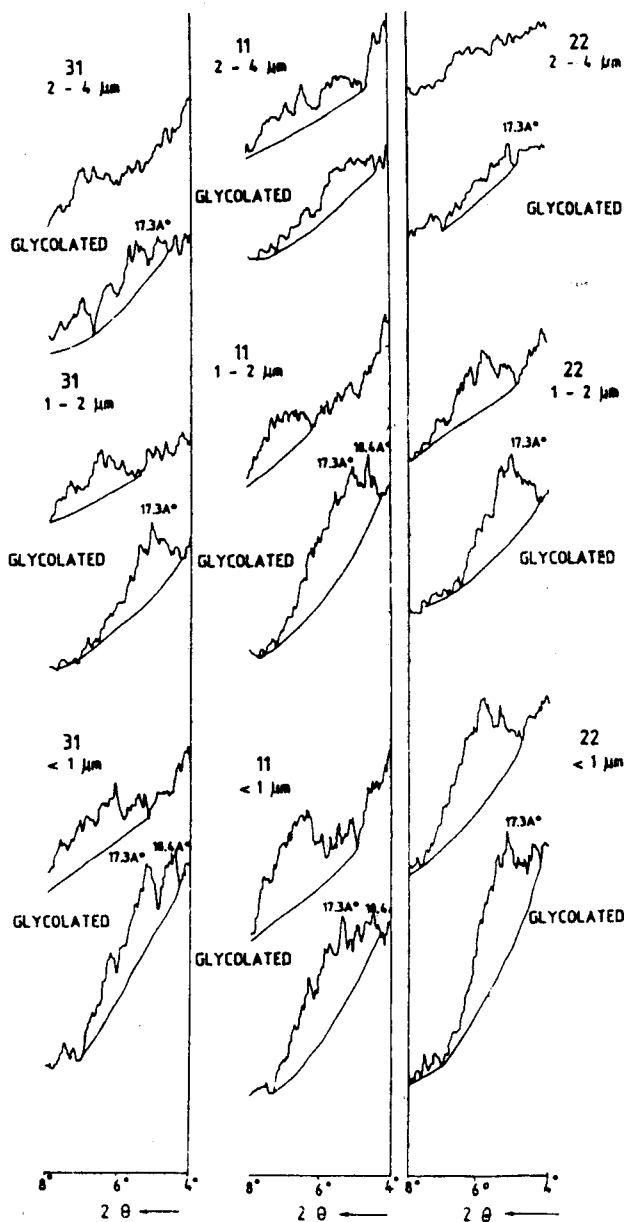


Fig. 2—X-ray patterns of montmorillonites in < 1 , 1-2 and 2-4 μm fractions

fractions < 1, 1-2 and 2-4 μm —IR spectra and glycolated X-ray diffractograms of different clay sizes (Figs 2-5) revealed 2 smectite minerals. The 17.3 \AA peak on glycolated X-ray diffractogram and characteristic absorption peaks at 3640 cm^{-1} (O-H stretching region) and $920, 878$ and 840 cm^{-1} (O-H bending region) in the infrared spectra¹⁵ observed here are ascribed to montmorillonite. Substitution of Al by Fe in the octahedral sites results in a progressive shift in the O-H bending vibration from $920\text{--}820\text{ cm}^{-1}$ and various combinations of Fe, Al and Mg result in intermediate values¹⁶. Absorption at $814\text{--}818\text{ cm}^{-1}$ has been assigned to $\text{Fe}^{3+}\text{--Fe}^{3+}$ -OH bending⁸. However for Fe-rich smectites, O-H stretching vibration shifts to lower frequency as compared to Al-rich smectites. Therefore, the characteristic absorption peaks observed at 3520 cm^{-1} and $815\text{--}812, 680$ and 600 cm^{-1} close to the peaks of nontronite and 18.4 \AA reflection in the glycolated X-ray diffractogram are ascribed to Fe-rich montmorillonite. In this work characteristic en-

dothermic peaks at about 150°C and 650°C are ascribed to Al-montmorillonite and endothermic peaks at about 150°C and 550°C are given to nontronite or Fe-rich montmorillonite^{17,18}.

Montmorillonite is present in all size fractions of the calcareous, siliceous and pelagic sediments. In addition to this montmorillonite, Fe-rich montmorillonite is present in < 1 μm and 1-2 μm fractions of the siliceous and < 1 μm fraction of the pelagic sediments. No Fe-rich montmorillonite is identified in calcareous sediments.

Percentage of 2 types of montmorillonites together is highest in < 1 μm fraction, followed by 1-2 μm and 2-4 μm fraction (Fig. 2) and least in 2-4 μm fraction (Figs 2 and 6).

V/P value (Fig. 2) of montmorillonite is highest (0.59) in calcareous sediments followed by siliceous (0.43) and pelagic sediments (0.4). It indicates that the montmorillonites in calcareous sediments are more crystalline than in siliceous and pelagic sediments. Average V/P of montmorillonite is highest

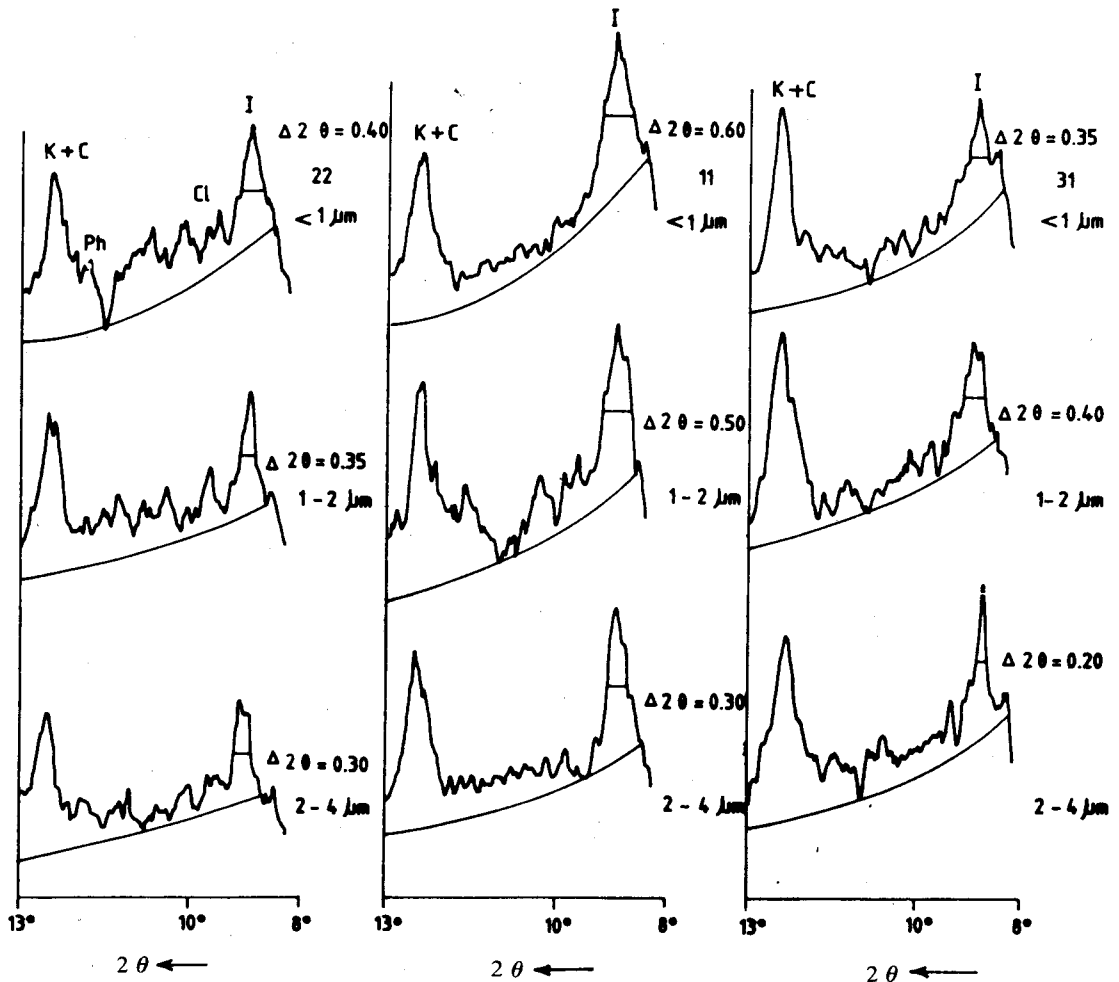


Fig. 3—X-ray diffractograms of illite and kaolinite + chlorite in < 1, 1-2 and 2-4 μm fractions

(0.53) in 1-2 μm fraction of all types of sediments compared to 0.44 in $< 1 \mu\text{m}$ fraction and 0.4 in 2-4 μm fraction. It shows that the montmorillonite in 1-2 μm size fraction is more crystalline compared to the montmorillonite in < 1 and 2-4 μm fractions.

Percentage of illite increase with an increase in particle size of the sediment (Fig. 6). Highest crystallinity of illite is found in pelagic clays followed by calcareous and siliceous sediments and as far as the size fractions are concerned the highest crystallinity is in 2-4 μm fraction followed by 1-2 μm and $< 1 \mu\text{m}$ size fractions. $\Delta 2\theta$ (Fig. 3) of illite decreases with increasing size fraction. It indicates that the crystallinity of illite is highest in 2-4 μm fraction followed by 1-2 and $< 1 \mu\text{m}$.

Kaolinite + chlorite are identified by their common basal reflections at 7 \AA and 3.54 \AA from the X-ray diffractograms and from the characteristic

peaks at $3670, 3650, 915$ and 785 cm^{-1} for kaolinite and $3560, 3150, 950$ and 760 cm^{-1} for chlorite from the infra-red spectra. An attempt to separate kaolinite and chlorite by slow scan method¹⁹ failed because the zeolites are present in all size fractions with varying abundance. The (020) reflection of phillipsite and (050) reflection of clinoptilolite interfere with the combined reflections of kaolinite and chlorite at 7.0 \AA and 3.54 \AA respectively. Therefore the percentage of kaolinite + chlorite is calculated in all size fractions. Percentage of kaolinite + chlorite estimated on 7.0 \AA reflection indicates that it increases with increasing size fraction (Fig. 6).

Discussion

Distributional patterns of illite, kaolinite + chlorite in $< 2 \mu\text{m}$ fraction reveal that the concentrations of these minerals are higher in the northern part of

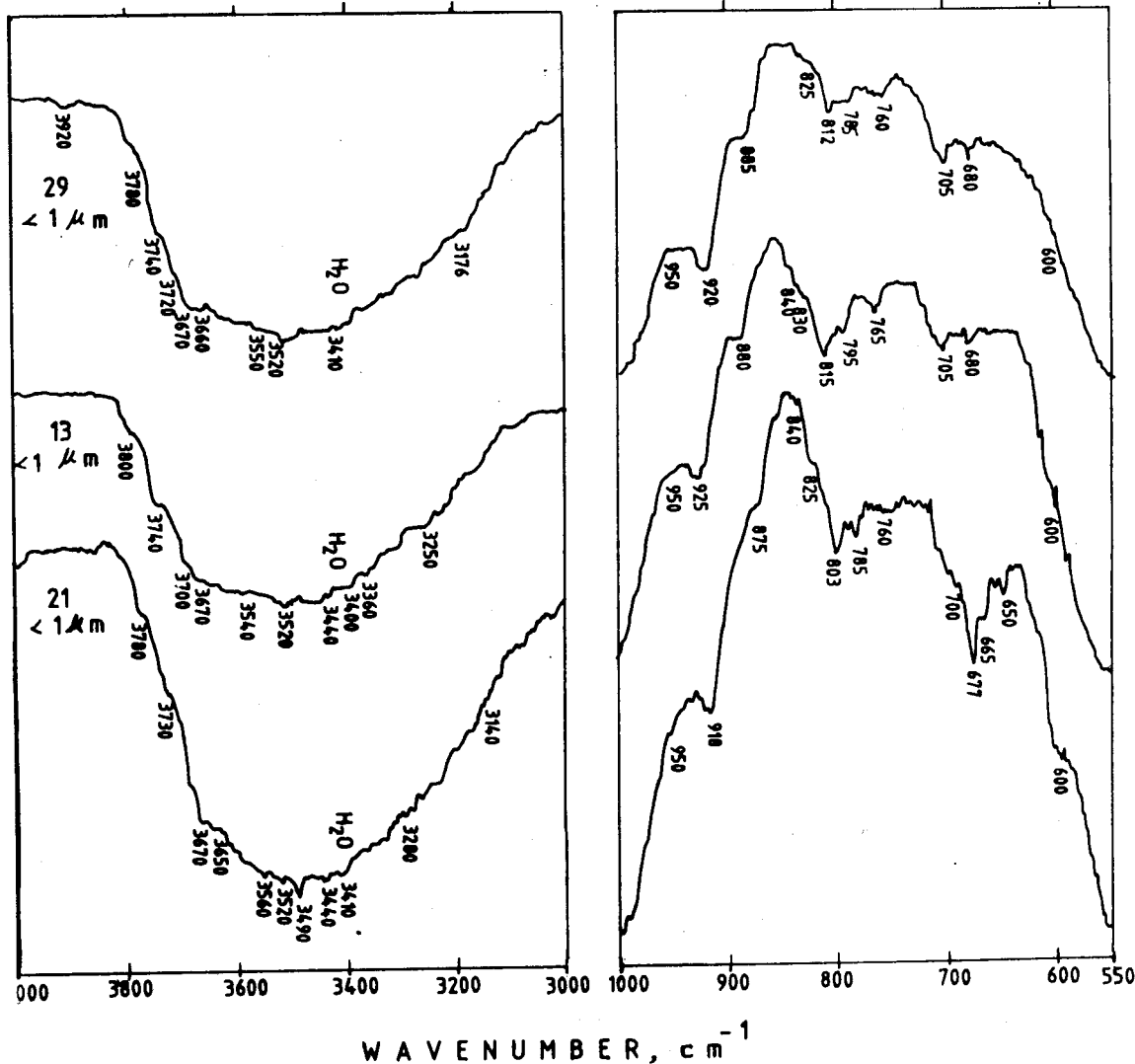


Fig. 4—IR spectra of $< 1 \mu\text{m}$ fraction of sediments (21: calcareous sediment, 13: siliceous sediment and 29: pelagic clay)

the basin (areas 1 and 2) and they decrease in the southern part of the basin (area 4) towards pelagic clay. It confirms that there is a continental flux into the basin from north, which may be from Ganges and Brahmaputra river discharge²⁰⁻²³ that have been transported by turbidity currents and subsequently deposited in the basin⁵. Distributional pattern of montmorillonite suggests that there are large variations in abundance of this mineral within the basin and also within different sediment facies. It is also observed that the concentrations of montmorillonite are inversely proportional to illite percentage. The higher concentration of montmorillonite in this basin may be due to the weathering of ridge rocks which contain basic volcanic material. This inference gains support by the presence of higher degree of crystallinity of montmorillonite in all size fractions of calcareous sediments which are from the adjacent ridge rocks. In addition to montmorillon-

ite, Fe-rich montmorillonite is present in < 1 and 1-2 μm fractions of the siliceous and 1 μm fraction of the pelagic clays. Fe-rich montmorillonite may have formed by the interaction between iron hydroxides and biogenic silica in the sediments during early diagenesis²⁴. This mechanism may be expected in siliceous sediments where high content of biogenic silica is present. In pelagic sediments however, Fe-rich montmorillonite is found in < 1 μm fraction which may be due to the presence of Opal-CT observed in these sediments when the samples were heated to 900°C for 1 h. Absence of Fe-rich montmorillonite in calcareous sediments may indicate that there is no or less diagenetic process takes place in these sediments. This may be due to higher biogenic sedimentation which is inhibiting this process. Rao²⁵ observed that the polymetallic nodules associated with siliceous sediments contain lesser concentrations of iron than Mn and the nodules as-

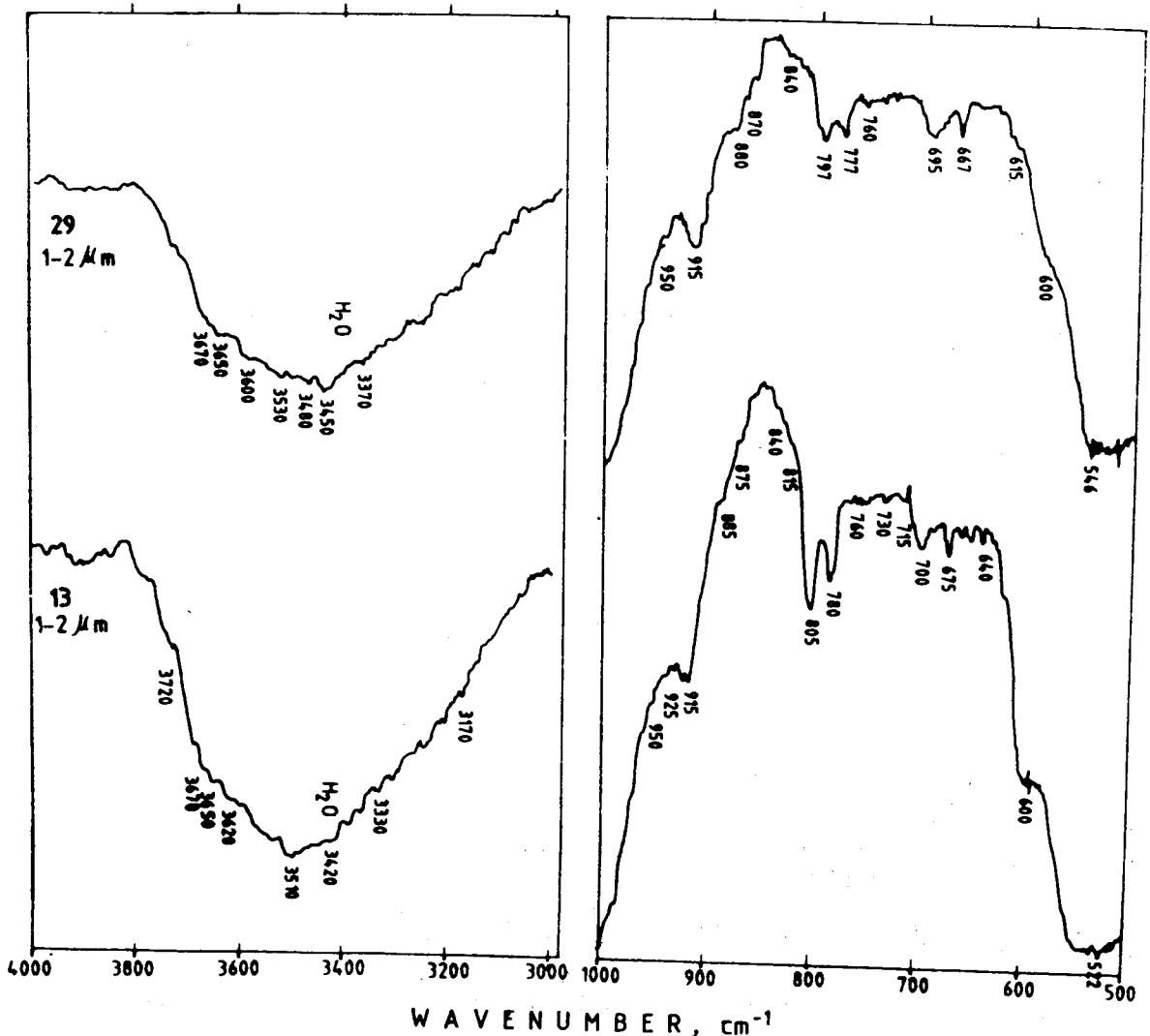


Fig. 5—IR spectra of 1-2 μm fraction of sediments

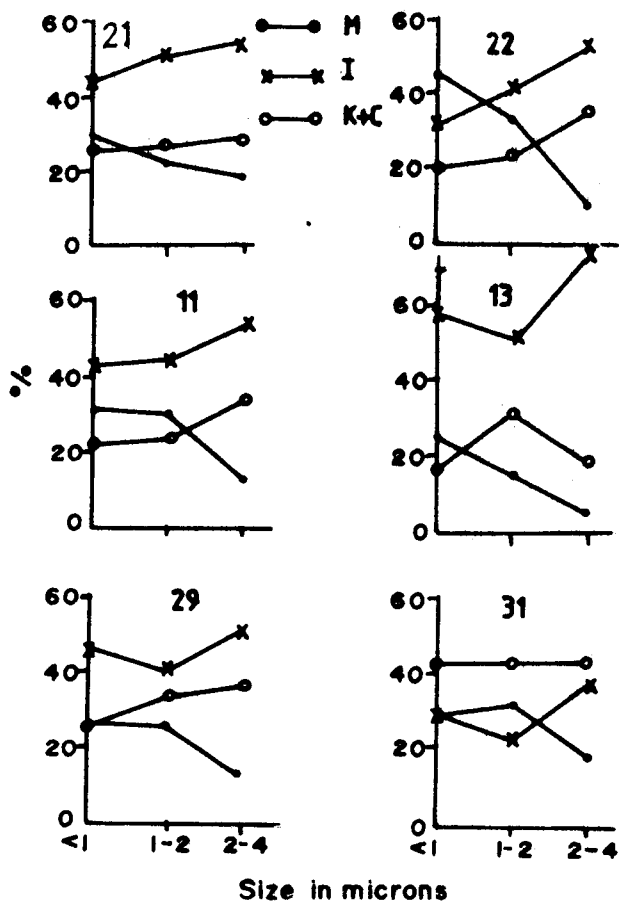


Fig. 6—Distribution of montmorillonite (M), illite (I) and kaolinite + chlorite (K + C) in < 1, 1-2 and 2-4 μm fractions

sociated with pelagic clay contain higher concentrations of Fe than Mn. It further confirms that more Fe content is utilised in the formation of Fe-rich montmorillonite in siliceous sediments thus leaving free Mn to form todorokite-rich nodules. Processes similar to, have been reported from equatorial Pacific⁷ and in Bauer Deep⁸. More content of montmorillonite in < 1 and 1-2 μm fractions compared to 2-4 μm fraction suggest that unlike the other clay minerals, montmorillonite tends to crystallise and size segregate in these fractions. Percentage of illite increases with increasing size fraction (Fig. 6). It may be because the montmorillonite content is decreasing with the increasing size fraction and weighting factor 4 has been used in the estimation of illite percentage. In reality illite is also reducing with increasing size fraction (Fig. 3). Lowest crystallinity of illite in finer fractions may be due to the effect of early diagenesis in these sediments.

Acknowledgement

The authors thank late Dr H N Siddiquie, former Director, Dr B N Desai, Director and Mr P S N Murty for encouragement. Thanks are due to Mr R R Nair for valuable suggestions, and to Drs S K Paknikar and Kamat Dalal of Goa University for IR spectrophotometer and DTA facilities. This work was carried out with the financial support of Department of Ocean Development, New Delhi.

References

- 1 Griffin J J, Wisdom H & Goldberg E D, *Deep-Sea Res*, **15** (1968) 433.
- 2 Rateev M A, Gorbunova Z N, Lisitzin A P & Nosov G L, *Sedimentology*, **13** (1969) 21.
- 3 Goldberg E D & Griffin J J, *Deep-Sea Res*, **17** (1970) 513.
- 4 Kolla V & Biscaye P E, *Deep-Sea Res*, **20** (1973) 727.
- 5 Kolla V, Henderson L & Biscaye P E, *Deep-Sea Res*, **23** (1976) 949.
- 6 Bischoff J L & Rosenbaun R J, *Earth Planet Sci Lett*, **33** (1977) 379.
- 7 Hein J R, Yeh H W & Alexander E, *Clays & Clay Minerals*, **27** (1979) 185.
- 8 Cole T G, *Geochim Cosmochim Acta*, **49** (1985) 221.
- 9 Whitehouse U G, Jeffrey L M & Debbrecht J D, *Clays and clay minerals (Proceedings of 7th national conference)* edited by A Swineford (Pergamon Press, London) 1960, 79.
- 10 Folk R L, *Petrology of sedimentary rocks* (Hemphills, Austin) 1965, 177.
- 11 Brindley G W & Brown G, *Crystal structures of clay minerals, their X-ray identification*, (Mineralogical Society, London) 1980, 496.
- 12 Biscaye P E, *Geol Soc Am Bull*, **76** (1965) 803.
- 13 Kitch H J, *J Geol Soc Lond*, **137** (1980) 271.
- 14 Chester R & Elderfield H, *Chem Geol*, **12** (1973) 281.
- 15 Van der Marel & Beutel Spacher H, *Atlas of infrared spectroscopy of clay minerals and their admixtures* (Elsevier Sci Pub Co, Amsterdam) 1976, 396.
- 16 Farmer V C & Russel J D, *Clays & Clay Minerals*, **15** (1967) 121.
- 17 Aoki S, Kohyama N & Sudo T, *Deep-Sea Res*, **21** (1974) 865.
- 18 Aoki S, Kohyama N & Sudo T, *Deep-Sea Res*, **26A** (1979) 893.
- 19 Biscaye P E, *Am Miner*, **49** (1964) 1281.
- 20 Rama Murthy M & Srivastava P C, *Mar Geol*, **33** (1979) M21.
- 21 Subramanian V, *Mar Geol*, **36** (1980) M29.
- 22 Rao V P, Reddy N P C & Rao Ch M, *Cont shelf Res*, **8** (1988) 151.
- 23 Naidu A S, Mowatt T C, Somayajulu B L K & Rao K S, *Scope/UNEP Sunderband Heft 58*, (Mitt Geol Paleont Inst, Univ Hamburg) 1985, 559.
- 24 Lyle M, Dymond J & Heath G R, *Earth Planet Sci Lett*, **35** (1977) 55.
- 25 Rao V P, *Mar Geol*, **74** (1987) 151.